JACS
JOURNAL OF THE AMERICAN CHEMICAL SOCIETY

Communication

pubs.acs.org/JACS

Stepwise Assembly of $Pd_6(RuL_3)_8$ Nanoscale Rhombododecahedral Metal–Organic Cages via Metalloligand Strategy for Guest Trapping and Protection

Kang Li,[†] Lu-Yin Zhang,[†] Cheng Yan,[†] Shi-Chao Wei,[†] Mei Pan,*[,†] Li Zhang,[†] and Cheng-Yong Su*[,†,‡]

[†]MOE Laboratory of Bioinorganic and Synthetic Chemistry, State Key Laboratory of Optoelectronic Materials and Technologies, Lehn Institute of Functional Materials, School of Chemistry and Chemical Engineering, Sun Yat-Sen University, Guangzhou 510275, China

[‡]State Key Laboratory of Applied Organic Chemistry, Lanzhou University, Lanzhou 730000, China

Supporting Information

ABSTRACT: Stepwise synthesis of nanosized Pd–Ru heteronuclear metal–organic cages from predesigned redox- and photo-active Ru(II)-metalloligand and naked Pd(II) ion is described. The resulting cage shows rhombododecahedral shape and contains a 5350 Å^3 cavity and 12 open windows, facilitating effective trapping of both polar and nonpolar guest molecules. Protection of photosensitive guests against UV radiation is studied.

The design and synthesis of metal–organic cages (MOCs) with well-defined shapes and cavities have received wide attention during the past decades, originating in host–guest chemistry but now triggering interest in catalytic and biological applications.[1] Among them, selective encapsulation of guest compounds by discrete, nanoscale cages has been applied to various tasks such as molecular catalysis,[2] hazardous chemicals capture,[3] reactive intermediates stabilization,[4] and drug delivery and release,[5] as well as to detecting or sensing systems.[6] By applying various synthetic strategies such as "symmetry interaction", "directional bonding", "molecular paneling", and "molecular clips", a number of MOCs with varied structure and property attributes are fabricated.[1] So far, most of the MOCs involve homoleptic mononuclear or dimetallic unit centers[7] featuring specific coordination geometry. In contrast, heterometallic ensembles of discrete metallosupramolecular cages, despite the anticipation that incorporating multiple metal centers may endow novel physical properties and more functions, are still in their infancy. To achieve this synthetic goal, the intricate behaviors among multivariate coordination geometries of polynuclear metal centers must be balanced, and this is a particular challenge to actualize in a one-pot reaction.[8]

An alternative method is to use a stepwise approach by applying predesigned building blocks known as metalloligands.[9] This strategy incorporates metal complexes with "free" donor groups for further metal binding in lieu of simple organic ligands, which has been proven effective in introducing rich spectroscopic, catalytic, or magnetic features, in addition to providing the ability to construct intricately designed discrete or infinite structures. In this context, coordination species containing a variety of transition metals (Ru, Ir, Pt, Re, Ti, Zn, Cu, Fe) are preconstructed as metalloligands for further fabrication of infinite metal–organic frameworks (MOFs).[10] Especially, incorporating Ir(III) or Ru(II)/(III) ions into metalloligands can bring rich redox or opto-electronic activities and show potential applications in fields like photocatalysis.[11] However, reports of discrete heteronuclear MOCs that involve the use of metalloligands are still limited.[12] Our group has been interested in developing robust MOCs by integrating potential active sites, such as Cu^+ and Ag^+.[2b,13] Herein, we report stepwise assembly of nanosized heterometallic Pd(II)–Ru(II) MOCs by using a predesigned bulky triangular Ru(II)-metalloligand.

Scheme 1. Synthetic Route for the Ru(II)-Metalloligand RuL_3 and $Pd_6(RuL_3)_8$ Metal–Organic Cage Showing Guest Encapsulation

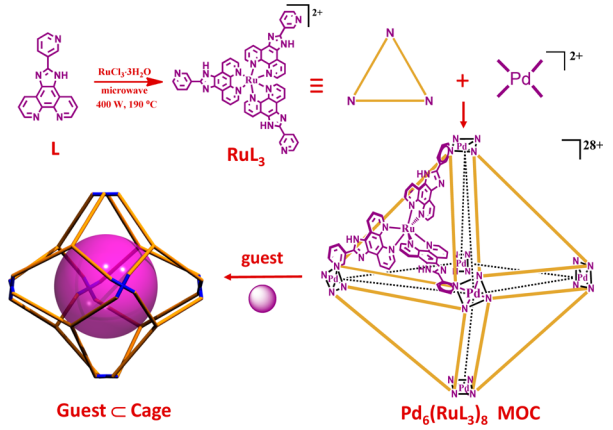

As illustrated in Scheme 1, combination of the spatially triangular C_3 symmetry of RuL_3 metalloligand with the coplanar-squared D_4 symmetry of the naked Pd(II) center is expected to result in convergent formation of a $Pd_6(RuL_3)_8$ MOC, with 6 Pd occupying the vertices of a truncated octahedron and 8 RuL_3 lying on the faces (assignable to rhombododecahedron, *vide infra*). Applying Ru-metalloligand containing strongly bonded aromatic and heterocyclic backbones can not only provide well-oriented coordination sites to easily control the assembly of the target cage structure but also favor shielding and $\pi-\pi$ interactions with guest molecules. Furthermore, the opto-

Received: September 30, 2013
Published: March 10, 2014

   dx.doi.org/10.1021/ja410044r | J. Am. Chem. Soc. 2014, 136, 4456–4459

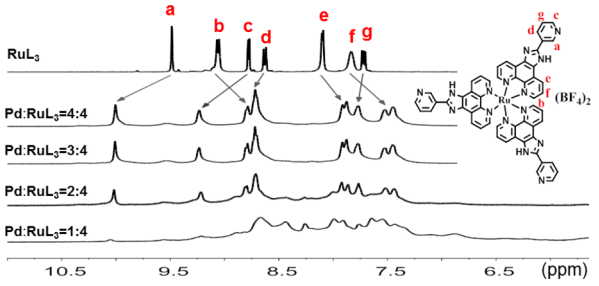

Figure 1. ^{1}H NMR titration of metalloligand $RuL_3(BF_4)_2$ (top) with $Pd(BF_4)_2$ in a mixture of DMSO-d_6/D_2O (1:2 v:v). Shifts of the proton peaks in $Pd_6(RuL_3)_8(BF_4)_{28}$ are shown by arrows.

electrical character and aqueous-solution compatibility of Ru complexes may give the cage special usefulness from chemical and biological points of view. In this Communication, encapsulation of polar and nonpolar guests and protection of photosensitive molecules are shown.

The triangular metalloligand RuL_3X_2 (X = PF_6^-, BF_4^-, or NO_3^-), possessing 3 coordinated phenanthroline moieties and 3 uncoordinated pyridine (Py) pendants, was prepared by reaction of L with $RuCl_3{\cdot}3H_2O$ in a microwave method, and was further assembled with Pd(II) salts at 80 °C to result in formation of cage structures $[Pd_6(RuL_3)_8]X_{28}$·solvents (X = BF_4^- or NO_3^-, see SI). The solution assembly process was monitored by means of ^{1}H NMR titration in a DMSO-d_6/D_2O mixture (Figure 1). In general, the proton signals of pure RuL_3 metalloligand are well discriminable, while those of cage motifs are remarkably broadened due to slow rotational diffusion and dynamics typical of large molecules. Upon addition of $Pd(BF_4)_2$ into a solution of $RuL_3(BF_4)_2$, new proton signals appeared besides those of "free" RuL_3 ligand. This clearly indicates complexation between RuL_3 and Pd(II) ions, and the metal–ligand exchange is slow enough to be distinguished in the NMR time scale. At low Pd(II) concentration (Pd:RuL_3 = 1:4), the spectra display a number of unsolved signals, indicative of diversification of the coordination assembly. Upon increasing the Pd:RuL_3 ratio to 2:4 and 3:4, the proton peaks become unified, turning to a set of well-resolved signal patterns. This suggests the coordination assembly converges on formation of a thermodynamically preferential $Pd_6(RuL_3)_8$ cage, which is stable enough even in an excess of Pd(II) ions (Pd:RuL_3 = 4:4). The 7 proton peaks of the $Pd_6(RuL_3)_8$ cage show diverse shifts relative to those of the free RuL_3 metalloligand. The signals of Py H-atoms (a,c,d,g) are moved downfield, obviously due to coordination of the Py-donor to Pd(II) that gives a metal-induced effect.[13] In contrast, the signals of phenanthroline H-atoms (b,e,f) are moved upfield due to formation of the $Pd_6(RuL_3)_8$ cage, where the H-atoms on the phenanthroline moieties are subject to arene ring shielding. The assignments of these peaks are verified carefully by ^{1}H–^{1}H COSY spectra, which clearly establish proton correlation (Figures S1 and S2).

To further elucidate the solution structure of the $Pd_6(RuL_3)_8$ cage, high-resolution electrospray ionization time-of-flight mass spectrometry (HR-ESI-TOF-MS) was performed. As can be seen from Figure 2, a series of $Pd_6(RuL_3)_8$ cage species possessing successive valence states can be identified from the m/z 750–1500 range. For example, the peak at m/z 1133.3672 is assignable to the octavalent $[Pd_6(RuL_3)_8{-}12H^+)^{16+}{+}8(NO_3^-)]^{8+}$ motif, which is verified by precise matching of experimental and simulated data (Figure S4). It is noticed that there are a total of 24 NH protons on the cage, which are apt to

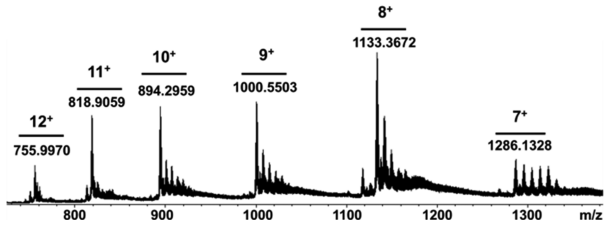

Figure 2. HR-ESI-TOF-MS spectra of $[Pd_6(RuL_3)_8](NO_3)_{28}$ cage species in DMSO–CH_3CN (1:20 v:v) solution.

dissociate under MS conditions. Detailed analyses of the HR-ESI-TOF-MS peaks of observed $Pd_6(RuL_3)_8$ cage species of different valence states are given in Figure S4.

The unambiguous cage structure was disclosed by single-crystal X-ray diffraction. We succeeded in cocrystallizing the $Pd_6(RuL_3)_8$ cage with a heavy coordination molecule, Ir(ppy)$_2$(bpyac) (ppy = 2-phenylpyridine, bpyac = 2,2′-bipyridine-4,4′-dicarboxylic acid), obtaining red crystals of $[Pd_6(RuL_3)_8][Ir(ppy)_2(bpyac)]_4(NO_3)_{24}$·solvents suitable for X-ray analysis. The results confirm that the cage consists of 6 Pd ions and 8 RuL_3 metalloligands, with Ir(III) complex units staying outside. As shown in Figures 3 and S3, each RuL_3

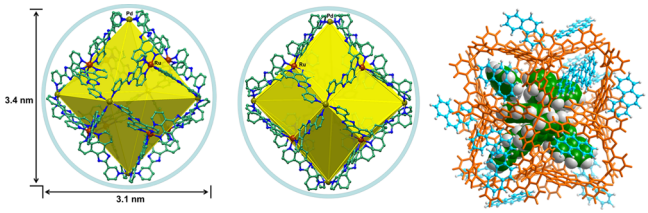

Figure 3. Crystal structures of $Pd_6(RuL_3)_8$ MOCs showing cage shape as truncated octahedron (left) and rhombododecahedron (middle), and MD simulation (right) showing maximum Phen guests uptake inside (space-filling mode) and in the doorway (stick mode) of the cage.

metalloligand comprises 1 octahedral RuN_6 center and 3 L's coordinated via 6 phenanthroline N-atoms, forming a spatially trigonal geometry. Coordinating the terminal Py N-donors to square-planar Pd ions accomplishes assembly of a truncated-octahedral cage, with 8 RuL_3 metalloligands occupying the 8 faces and 6 PdN_4 planes truncating the 6 vertices of the octahedron. This cage possesses 12 rhombic windows alongside each octahedral edge, so the cavity and windows of this cage can

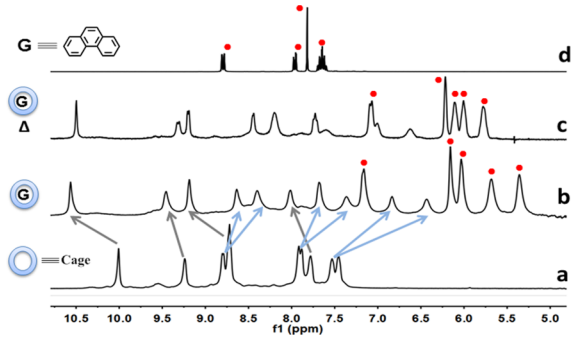

Figure 4. ^{1}H NMR study of guest inclusion by $Pd_6(RuL_3)_8$ MOC: (a) free cage, (b) PhenCcage at room temperature and (c) at 80 °C in a mixture of DMSO-d_6/D_2O (1:2 v:v), and (d) free Phen in DMSO-d_6. Signals of guests are marked with red dots. The arrows show shifts and splitting of Py-H (gray) and Phen-H (blue) on the cage.

dx.doi.org/10.1021/ja410044r | J. Am. Chem. Soc. 2014, 136, 4456–4459

be more accurately described as a rhombododecahedron, simply by connecting 6 Pd-atoms and 8 Ru-atoms. The overall cage size is estimated to be 3.1×3.4×3.4 nm^3, possessing 6 Pd vertices with separation of 27.9, 29.5 and 29.5 Å and a large cavity of 5350 $Å^3$. The cage size in solution was also estimated by DOSY analysis (Figure S5). It is evident that the 7 proton signals of the $Pd_6(RuL_3)_8$ cage display almost identical diffusion coefficients (D). According to the Stokes−Einstein equation (see SI), the dynamic radius of the cage was approximated as 16 Å, which is in accordance with the single-crystal structural analysis result (34/2 = 17 Å).

The large hydrophobic cavity and relatively narrow windows of the Pd−Ru cage inspire us to test its guest inclusion behavior in water-containing hydrophilic solvent, taking advantage of the known hydrophobic effect.[2d,6b−d] The neutral nonpolar and water-immiscible aromatics with increasing sizes from phenanthrene (Phen) to pyrene, anthracene, and perylene were first explored (Figures 4, S6−S15, and details in SI). Figure 4 presents the ^{1}H NMR monitoring of Phen encapsulation. In comparison to spectra of free host and guest, the striking finding of the guests⊂cage system is that the proton peaks belonging to guest molecules move significantly upfield, while those of the cage split from 7 to 10. Detailed analysis unveils the fact that protons on the Py moiety are shifted downfield, while those on the phenanthroline moiety are further split and upfield-shifted (Figure 4b). These observations definitely confirm trapping of guests and formation of noticeable interactions between host and guests, because encapsulation of aromatic guests is expected to form proper $\pi-\pi$ interactions with the face phenanthroline moieties rather than the corner Py moieties. Furthermore, integration of proton peaks and NMR/DOSY titration tests suggest that ∼18 ± 2 Phen guest molecules could be trapped by one cage in a stepwise manner (Figures S7 and S8). To deeply understand the loading positions and maximum uptake of the guest molecules, molecular dynamics (MD) simulation was performed (see SI). The simulation results reveal that a maximum of 7 Phen molecules can reside in the cavity of the coordination cage, while another 17 Phen guests can be accommodated in the doorway of 12 cage windows (Figure 3), allowing as many as 24 Phen guests in total to be trapped. From crystal structure we know the cage windows consist of $Pd_2Ru_2L_4$ motifs, where 4 bulky L motifs actually make up an open "box" to be able to hold in Phen guests via $\pi-\pi$ interactions. Such a versatile guest inclusion mode was further testified by DOSY measurements (Figures S6 and S8), in which the diffusion coefficients for both $Pd_6(RuL_3)_8$ cage and all Phen guests are identical, clearly confirming close host−guest association and giving a dynamic radius of the guests⊂cage ensemble of 18 Å. Upon heating of the sample to 80 °C, the H signal patterns become simplified with converging of some splitting peaks, apparently due to faster MD and weakening of host−guest interactions (Figure 4c).

Similar guest inclusion behaviors are also found for a bit larger pyrene or longer anthracene. As shown in Figures S9−S12, inclusion of pyrene or anthracene leads to remarkable broadening and shifting of H signals on both host and guest molecules. However, elevating the temperature to 80 °C gives rise to sharper and well-resolved signal profiles, unambiguously correlating with the host cage and guest pyrene or anthracene. Again, all guest proton peaks display clear upfield shifts, showing an arene ring-shielding effect by the host cage. According to integration of the H peaks, an average of 12 pyrene or anthracene molecules can be trapped by each $Pd_6(RuL_3)_8$ cage. In contrast, when aromatic molecules of even larger size, like perylene, were tested, no obvious guest inclusion behavior was detected (Figures S13−S15). This denotes a size selectivity of the $Pd_6(RuL_3)_8$ cage for guest inclusion. The rhombic windows of the cage seem not adequate for free passing of the bulky perylene guest.

The ability to trap and stabilize photosensitive molecules by this inherently redox- and photo-active MOC was tested for three photoinitiators, 2,2-dimethoxy-2-phenylacetophenone (DMPA), 1-hydroxycyclohexyl phenyl ketone (HCPK), and 2-hydroxy-2-methylpropiophenone (HMPP), which are light-curing agents widely used in ink and paint. As can be seen from Figures 5, S16, and S17, trapping of these photosensitive

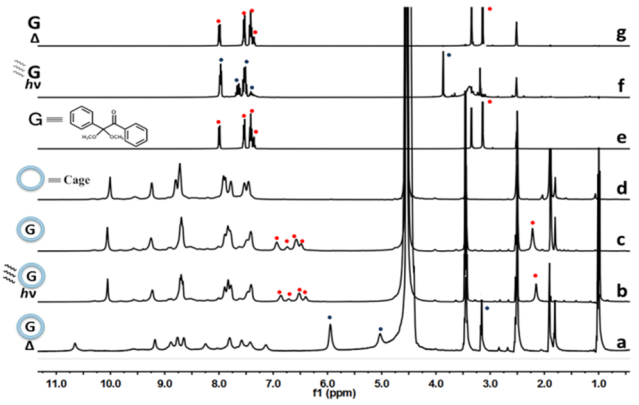

Figure 5. ^{1}H NMR spectra of photosensitive DMPA molecule, pure $Pd_6(RuL_3)_8$ MOC, and guest⊂cage systems under different conditions: (a−c) guest trapping by $Pd_6(RuL_3)_8$ cage measured in DMSO-d_6/D_2O (1:2 v:v) after heating at 80 °C for 24 h and then cooling to room temperature (a), after exposure to radiation of 365 nm UV light for 12 h (b), and as trapped (c). (d) Pure $Pd_6(RuL_3)_8$ cage. (e−g) DMPA measured in DMSO-d_6: (e) as purchased, (f) after exposure to radiation of 365 nm UV light for 12 h, and (g) after heating at 80 °C for 24 h and then cooling to room temperture. Signals relating to DMPA are shown by red (intact) or blue (decomposing) dots.

molecules by the $Pd_6(RuL_3)_8$ cage is convincing from ^{1}H NMR study, in which the proton peaks of free guest molecule move upfield after inclusion, indicative of cage shielding. In contrast to the above-discussed nonpolar aromatic guests, these photosensitive molecules are polar in nature and soluble in the DMSO/D_2O mixture; thus, there is rapid exchange between the inside and outside guests,[2d] as revealed by NMR/DOSY titration monitoring of the HMPP cage system (Figures S18−20). Compared to the inclusion behavior of aromatic guests, the cage protons are less affected upon inclusion of these photosensitive guests. However, increasing the solvent hydrophilicity can facilitate guest inclusion to lead to better trapping behavior under more aqueous environment (Figures S19 and S20).

The preliminary UV radiation study suggests a notable protective effect on these guest photoinitiators (Figures 5, S16, and S17). In general, upon radiation with 365 nm UV light for 12 h, the free molecules show photolysis while the trapped ones remain intact, which is recognizable in the ^{1}H NMR spectra. We carried out control experiments to explore the origin of this protective effect under comparable conditions by keeping the same molarity of the cage and metalloligand based on the RuL_3 unit (Figures S21−S23). The results indicate that the pure RuL_3 metalloligand itself can shield these photosensitive molecules from UV radiation, indicative of photoprotection originating from the RuL_3 ligand; however, the cage systems can protect the photosensitive guests on an even longer time scale. Photolysis

dx.doi.org/10.1021/ja410044r | J. Am. Chem. Soc. 2014, 136, 4456−4459

appears after 24 h in the presence of pure RuL_3, while it is suppressed using the $Pd_6(RuL_3)_8$ cage up for 120 h. Photoprotective ability of pure RuL_3 decreases in the order DMPA > HCPK > HMPP. This makes such cages useful as photosensitive guest protectors. On one hand, the photoprotective cage is beneficial for the storage of photoinitiators and modulation of their photoinduced reactivity. For example, the photoshielding effect is useful in delaying photopolymerization to guarantee the required initiation time for photocuring materials, leaving a time window for fitting or embossing operation before complete curing, or lowering the curing rate and reducing stress shrinkage, with potential use in light-cured dental materials.[14] On the other hand, by imparting photoprotection to the encapsulated guests, the $Pd_6(RuL_3)_8$ cage can act as a potential container and "Trojan horse" of photosensitizers applicable in drug delivery and photodynamic therapy, which has been achieved by other Ru–organometallic cages.[4c,d] The photoprotective mechanism[15] may relate to the ultrafast photophysical dynamics of Ru complexes, which have wide adsorption in both the UV and visible regions and phosphorescence around 600 nm (Figures S24–S28), or it may arise from collisional quenching with metal ions acting as the quencher, which needs further investigation in depth.

Although these photoinitiators are thermally stable in free form, it is worth noting that the guests⊂cage systems undergo thermolysis upon heating to 80 °C for 24 h based on the NMR and MS detections (Figures 5, S16, and S17). A final thermal decomposition product of DMPA was successfully isolated and identified as benzil (Figures S29 and S30), indicating potential hydrolysis of acetal catalyzed by Lewis acids (possibly Pd ions) liberated under heating condition. However, thermolysis behaviors of HCPK and HMPP guests are not clear yet. Detailed studies of the heat and light effects on these host–guest systems with regard to reaction mechanism are in progress.

In conclusion, heterometallic Pd–Ru MOCs in the rare shape of a rhombododecahedron are assembled from metalloligands in a stepwise method. The large cage cavity and rhombic boxlike windows facilitate size-selective guest encapsulation and versatile trapping behaviors for polar and nonpolar guests, endowing the cage with the ability to transfer water-insoluble guests into a hydrophilic environment for possible drug delivery and reactivity purposes. Preliminary inclusion tests on photosensitive guest molecules against UV light radiation confirm the cage offers better photoprotection than the pure RuL_3 metalloligand, suggesting that such redox- and photo-active coordination cages can well shield the guests to prevent undesired photolysis, which is useful in preserving photosensitive substrates or, further, controlling and modulating their photocatalytic reactions.

■ ASSOCIATED CONTENT

Supporting Information

Synthesis and characterization details. This material is available free of charge via the Internet at http://pubs.acs.org.

■ AUTHOR INFORMATION

Corresponding Author

panm@mail.sysu.edu.cn; cesscy@mail.sysu.edu.cn

Notes

The authors declare no competing financial interest.

■ ACKNOWLEDGMENTS

This work was supported by the 973 project (2012CB821701), NSFC (Grants U0934003, 91222201, 21373276, 21121061, 21173272), and the RFDP of Higher Education of China. We also thank Mr. Chun-Ting He for help with MD simulations.

■ REFERENCES

(1) (a) Chakrabarty, R.; Mukherjee, P. S.; Stang, P. J. *Chem. Rev.* **2011**, *111*, 6810. (b) Amouri, H.; Desmarets, C.; Moussa, J. *Chem. Rev.* **2012**, *112*, 2015. (c) Yoshizawa, M.; Klosterman, J. K.; Fujita, M. *Angew. Chem., Int. Ed.* **2009**, *48*, 3418. (d) Biros, S. M.; Yeh, R. M.; Raymond, K. N. *Angew. Chem., Int. Ed.* **2008**, *47*, 6062. (e) Oliveri, C. G.; Ulmann, P. A.; Wiester, M. J.; Mirkin, C. A. *Acc. Chem. Res.* **2008**, *41*, 1618. (f) Chen, C.-L.; Zhang, J. Y.; Su, C.-Y. *Eur. J. Inorg. Chem.* **2007**, 2997. (g) Cook, T. R.; Zheng, Y.-R.; Stang, P. J. *Chem. Rev.* **2013**, *113*, 734.

(2) (a) Leung, D. H.; Bergman, R. G.; Raymond, K. N. *J. Am. Chem. Soc.* **2007**, *129*, 2746. (b) He, Q.-T.; Li, X.-P.; Chen, L.-F.; Zhang, L.; Wang, W.; Su, C.-Y. *ACS Catal.* **2013**, *3*, 1. (c) Kilbas, B.; Mirtschin, S.; Scopelliti, R.; Severin, K. *Chem. Sci.* **2012**, *3*, 701. (d) Bolliger, J. L.; Belenguer, A. M.; Nitschke, J. R. *Angew. Chem., Int. Ed.* **2013**, *52*, 7958. (e) Weckhuysen, B. M. *Angew. Chem., Int. Ed.* **2009**, *48*, 4910.

(3) (a) Mal, P.; Breiner, B.; Rissanen, K.; Nitschke, J. R. *Science* **2009**, *324*, 1697. (b) Riddell, I. A.; Smulders, M. M. J.; Clegg, J. K.; Nitschke, J. R. *Chem. Commun.* **2011**, *47*, 457.

(4) (a) Ziegler, M.; Brumaghim, J.; Raymond, K. *Angew. Chem., Int. Ed.* **2000**, *39*, 4119. (b) Fiedler, D.; Bergman, R. G.; Raymond, K. N. *Angew. Chem., Int. Ed.* **2006**, *45*, 745. (c) Therrien, B. *Chem. Eur. J.* **2013**, *19*, 8378. (d) Schmitt, F.; Freudenreich, J.; Barry, N. P. E.; Juillerat-Jeanneret, L.; Süss-Fink, G.; Therrien, B. *J. Am. Chem. Soc.* **2012**, *134*, 754. (e) Smulders, M. M. J.; Nitschke, J. R. *Chem. Sci.* **2012**, *3*, 785.

(5) (a) Nguyen, T. D.; Liu, Y.; Saha, S.; Leung, K. C. F.; Stoddart, J. F.; Zink, J. I. *J. Am. Chem. Soc.* **2007**, *129*, 626. (b) Mal, P.; Schultz, D.; Beyeh, K.; Rissanen, K.; Nitschke, J. R. *Angew. Chem., Int. Ed.* **2008**, *47*, 8297. (c) Ma, Z.; Moulton, B. *Coord. Chem. Rev.* **2011**, *255*, 1623. (d) Lewis, J. E. M.; Gavey, E. L.; Cameron, S. A.; Crowley, J. D. *Chem. Sci.* **2012**, *3*, 778.

(6) (a) Han, M.; Michel, R.; He, B.; Chen, Y.-S.; Stalke, D.; John, M.; Clever, G. H. *Angew. Chem., Int. Ed.* **2013**, *52*, 1319. (b) Kang, S. O.; Llinares, J. M.; Day, V. W.; Bowman-James, K. *Chem. Soc. Rev.* **2010**, *39*, 3980. (c) Biros, S. M.; Bergman, R. G.; Raymond, K. N. *J. Am. Chem. Soc.* **2007**, *129*, 12094. (d) Samanta, D.; Mukherjee, P. S. *Chem. Commun.* **2013**, *49*, 4307. (e) Samanta, D.; Mukherjee, S.; Patil, Y. P.; Mukherjee, P. S. *Chem. Eur. J.* **2012**, *18*, 12322.

(7) (a) Cotton, F. A.; Lin, C.; Murillo, C. A. *Acc. Chem. Res.* **2001**, *34*, 759. (b) Power, N. P.; Dalgarno, S. J.; Atwood, J. L. *Angew. Chem., Int. Ed.* **2007**, *46*, 8601.

(8) Mahata, K.; Lal Saha, M.; Schmittel, M. *J. Am. Chem. Soc.* **2010**, *132*, 15933.

(9) (a) Przychodzeń, P.; Korzeniak, T.; Podgajny, R.; Sieklucka, B. *Coord. Chem. Rev.* **2006**, *250*, 2234. (b) Cho, S.; Ma, B. Q.; Nguyen, S. T.; Hupp, J. T.; Albrecht-Schmitt, T. E. *Chem. Commun.* **2006**, 2563.

(10) (a) Miguel, C.-L.; Eugenio, C.; Carlos, J. G.; Alejandra, S.-P. *Inorg. Chem.* **2006**, *45*, 5653. (b) Halper, S. R.; Do, L.; Stork, J. R.; Cohen, S. M. *J. Am. Chem. Soc.* **2006**, *128*, 15255.

(11) (a) Wang, C.; Dekrafft, K. E.; Lin, W. B. *J. Am. Chem. Soc.* **2012**, *134*, 7211. (b) Smulders, M. M. J.; Jiménez, A.; Nitschke, J. R. *Angew. Chem., Int. Ed.* **2012**, *51*, 6681.

(12) (a) Hiraoka, S.; Sakata, Y.; Shionoya, M. *J. Am. Chem. Soc.* **2008**, *130*, 10058. (b) Sakata, Y.; Hiraoka, S.; Shionoya, M. *Chem. Eur. J.* **2010**, *16*, 3318. (c) Kryschenko, Y. K.; Seidel, S. R.; Arif, A. M.; Stang, P. J. *J. Am. Chem. Soc.* **2003**, *125*, 5193.

(13) (a) He, Q.-T.; Li, X.-P.; Liu, Y.; Yu, Z.-Q.; Wang, W.; Su, C.-Y. *Angew. Chem., Int. Ed.* **2009**, *48*, 6156. (b) Su, C.-Y.; Cai, Y.-P.; Chen, C.-L.; Smith, M. D.; Kaim, W.; Loye, H. C. z. *J. Am. Chem. Soc.* **2003**, *125*, 8595.

(14) (a) Volz, M.; Ziener, U.; Salz, U.; Zimmermann, J.; Landfester, K. *Colloid Polym. Sci.* **2007**, *285*, 687. (b) Berzins, D. W.; Abey, S.; Costache, M. C.; Wilkie, C. A.; Roberts, H. W. *J. Dent. Res.* **2010**, *89*, 82.

(15) (a) Sun, Y.; Liu, Y.; Turro, C. *J. Am. Chem. Soc.* **2010**, *132*, 5594. (b) Szacilowski, K.; Macyk, W.; Drzewiecka-Matuszek, A.; Brindell, M.; Stochel, G. *Chem. Rev.* **2005**, *105*, 2647.